

Determination of Molecular Anisotropy in Thin Films of Discotic Assemblies Using Attenuated Total Reflectance UV–Visible Spectroscopy

Ware H. Flora,⁺ Sergio B. Mendes,* Walter J. Doherty, III,
S. Scott Saavedra, and Neal R. Armstrong*

Department of Chemistry, University of Arizona, Tucson, Arizona 85721

Received August 6, 2004. In Final Form: October 4, 2004

We report here an investigation of absorbance anisotropy in highly ordered, single bilayer (ca. 5.6 nm) Langmuir–Blodgett (LB) thin films of discotic liquid-crystalline phthalocyanines, using a recently introduced broad-band attenuated total reflectance (ATR) spectroscopic technique, capable of measuring dichroism in such films in the UV–visible optical region down to absorbances of ca. 0.003 absorbance units. On the basis of the ATR measurements of LB-deposited films, a thorough treatment was established to determine the ensemble average of the Cartesian components and the associated optical anisotropy of transition dipoles in the molecular film. In an effort to recover order parameters of molecular orientation, those results were interpreted with a circular dipole model, which is the expected model for the isolated molecule based on symmetry properties. We measured a strong dipole component normal to the film plane that cannot be explained in terms of a truly circular model, indicating that the molecular transition dipoles were perturbed upon aggregation. The utility of the experimental approach was further demonstrated by (a) investigating the effect of substrate modifiers (methyl- and phenyl-terminated silanes) on the ordering within the phthalocyanine film and (b) the effect of water immersion and re-annealing of the thin film on molecular ordering and optical anisotropy.

Introduction

Discotic (disk-shaped), liquid-crystalline organic materials that form columnar or rodlike aggregated assemblies with considerable long-range order and a narrow distribution of molecular tilt angles and azimuthal rotations are increasingly interesting as active layers in organic electronic devices, such as field-effect transistors (OFETs) and photovoltaics (OPVs).^{1–21} It is critical to the

performance of such devices that the organic materials have high, and ideally anisotropic, charge mobility (conductivity). Discotic liquid-crystalline materials (substituted phthalocyanines, hexabenzocoronenes (HBCs), triphenylenes, etc.) are potentially attractive candidates for this role because they typically exhibit much higher charge mobility along the column axis of the rodlike aggregate than perpendicular to the column. It is believed that these charge mobilities will be affected by the extent of cofacial overlap between disks within the column, and therefore the microscopic orientation of these disks is expected to influence charge mobility.^{1,8,17–21} Complementary spectroscopic, X-ray and neutron diffraction methods, and scanning probe microscopies are needed to characterize the orientation of these disks on substrates which mimic those encountered in electronic devices.^{4–8,17–19}

One interesting class of discotic materials are the octasubstituted phthalocyanines (Pc's) which have been exploited as OFET and OPV materials.^{1,21,24} We have

* Authors to whom correspondence should be addressed. E-mail: nra@u.arizona.edu (N.R.A.), sergiom@email.arizona.edu (S.B.M.). Tel: (520) 621–8242 (N.R.A.), (520) 621–6340 (S.B.M.).

⁺ Present Address: Tate & Lyle Food and Industrial Ingredients, Americas 2200 E. Eldorado St., Decatur, IL 62525

(1) Lemaur, V.; Da Silva Filho, D. A.; Coropceanu, V.; Lehmann, M.; Geerts, Y.; Piris, J.; Debije, M. G.; Van de Craats, A. M.; Senthilkumar, K.; Siebbeles, L. D. A.; Warman, J. M.; Bredas, J. L.; Cornil, J. *J. Am. Chem. Soc.* **2004**, *126*, 3271.

(2) van de Craats, A. M.; Warman, J. M. *Adv. Mater.* **2001**, *13*, 130.

(3) van de Craats, A. M.; Stutzmann, N.; Bunk, O.; Nielsen, M. M.; Watson, M.; Müllen, K.; Chanzy, H. D.; Sirringhaus, H.; Friend, R. H. *Adv. Mater.* **2003**, *15*, 495.

(4) Piris, J.; Debije, M. G.; Stutzmann, N.; van de Craats, A. M.; Watson, M. D.; Müllen, K.; Warman, J. M. *Adv. Mater.* **2003**, *15*, 1736.

(5) Tchegotareva, N.; Yin, X. M.; Watson, M. D.; Samori, P.; Rabe, J. P.; Müllen, K. *J. Am. Chem. Soc.* **2003**, *125*, 9734.

(6) Tracz, A.; Jeszka, J. K.; Watson, M. D.; Pisula, W.; Müllen, K.; Pakula, T. *J. Am. Chem. Soc.* **2003**, *125*, 1682.

(7) Kubowicz, S.; Pietsch, U.; Watson, M. D.; Tchegotareva, N.; Müllen, K.; Thünemann, A. F. *Langmuir* **2003**, *19*, 5036.

(8) Laursen, B. W.; Norgaard, K.; Reitzel, N.; Simonsen, J. B.; Neilsen, C. B.; Als-Nielsen, J.; Bjørnholm, T. *Langmuir* **2004**, *20*, 4139.

(9) Cornil, J.; Beljonne, D.; Calbert, J.-P.; Bredas, J.-L. *Adv. Mater.* **2001**, *13*, 1053.

(10) Noh, Y.-Y.; Kim, J.-J.; Yoshida, Y.; Yase, K. *Adv. Mater.* **2003**, *15*, 699.

(11) Bourgoin, J.-P.; Doublet, F.; Palacin, S.; Vandevyver, M. *Langmuir* **1996**, *12*, 6473.

(12) Fujiki, M.; Tabei, H.; Kurihara, T. *Langmuir* **1988**, *4*, 1123.

(13) Manno, D.; Rella, R.; Troisi, L.; Valli, L. *Thin Solid Films* **1996**, *280*, 249.

(14) Osburn, E. J.; Schmidt, A.; Chau, L. K.; Chen, S. Y.; Smolenyak, P.; Armstrong, N. R.; O'Brien, D. F. *Adv. Mater.* **1996**, *8*, 926.

(15) Smolenyak, P. E.; Osburn, E. J.; Chen, S. Y.; Chau, L. K.; O'Brien, D. F.; Armstrong, N. R. *Langmuir* **1997**, *13*, 6568.

(16) Smolenyak, P.; Peterson, R.; Nebesny, K.; Toerker, M.; O'Brien, D. F.; Armstrong, N. R. *J. Am. Chem. Soc.* **1999**, *121*, 8628.

(17) Zangmeister, R. A. P.; Smolenyak, P. E.; Drager, A. S.; O'Brien, D. F.; Armstrong, N. R. *Langmuir* **2001**, *17*, 7071.

(18) Donley, C. L.; Xia, W.; Minch, B. A.; Zangmeister, R. A. P.; Drager, A. S.; Nebesny, K.; O'Brien, D. F.; Armstrong, N. R. *Langmuir* **2003**, *19*, 6512.

(19) Xia, W.; Minch, B.; Carducci, M. D.; Armstrong, N. R.; *Langmuir* **2004**, *20*, 7998–8005.

(20) Donley, C. L.; Mendes, S. B.; Nebesny, K. W.; Armstrong, N. R. manuscript in preparation.

(21) Donley, C. L.; Zangmeister, R. A. P.; Xia, W.; Minch, B.; Drager, A.; Cherian, S. K.; LaRussa, L.; Kippelen, B.; Domercq, B.; Mathine, D. L.; O'Brien, D. F.; Armstrong, N. R. *J. Mater. Res.* **2004**, *19*, 2087–2099.

(22) Flora, W. Ph.D. Dissertation, University of Arizona, 2004.

(23) Minch, B. A.; Xia, W.; Donley, C. L.; Hernandez, R. M.; Carter, C.; Carducci, M. D.; Dawson, A.; O'Brien, D. F.; Armstrong, N. R. *Chem. Mater.* submitted for publication.

(24) Yoo, S.-Y.; Domercq, B.; Donley, C.; Carter, C.; Xia, W.; Minch, B. A.; O'Brien, D. F.; Armstrong, N. R.; Kippelen, B. *International Symposium Organic Materials and Nanotechnology*, SPIE volume 5215, Organic Photovoltaics IV, **2004**, pp 71–78.

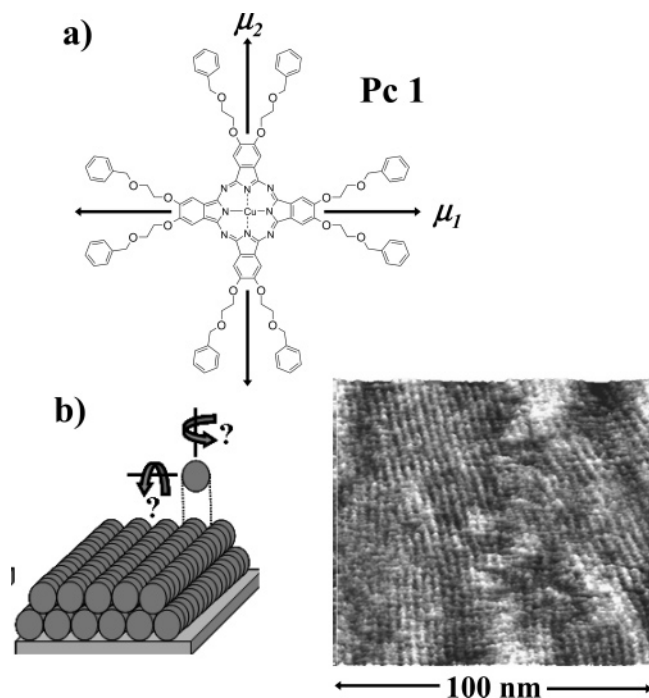


Figure 1. (a) Molecular structure of **Pc 1** and orientation of electronic transition dipoles with respect to the molecular structure for the isolated molecule, based on cited references. (b) AFM image of a bilayer of this molecule on hydrophobized silicon, demonstrating the formation of molecular columns, which can have coherence lengths over 200 nm long. Also shown is a model for such a bilayer, where the column alignment and stacking are known from previous reports but the specific tilt or rotation of the disks within the column is in question.

recently focused attention on octasubstituted alkoxy- and thioether-Pcs with benzyl-terminated side chains, e.g. 2,3,9,10,16,17,23,24-octakis(2-benzyloxyethoxy)phthalocyaninato copper(II) (abbreviated **Pc 1**; structure shown in Figure 1a),^{15–24} which have shown intriguing coherence and optical/electrical anisotropies as thin films. The bulk form of this Pc is liquid crystalline, with a transition temperature ($K \rightarrow LC$ mesophase) of ca. 68 °C.^{14,19,23} Recent studies have shown that this transition produces a hexagonal columnar mesophase structure, as with many alkoxy-based side-chain-modified discotic materials.²³ When films of **Pc 1** are compressed on a Langmuir–Blodgett (LB) trough, this material forms rigid bilayers of columnar assemblies, which run parallel to the compression barriers. These films can then be horizontally transferred to a substrate with high integrity, maintaining the alignment of the molecular columns. The AFM image and schematic in Figure 1b illustrates the alignment of these columns shown in previous work, with coherence up to ca. 200–300 nm for single columns.^{15–23} The full description of the optical anisotropy and molecular orientation within the column, however, is still lacking. Such aggregation produces a blue-shifted Q-band absorbance at ca. 625 nm relative to the monomer absorbance at ca. 690 nm.^{7,8,16–21}

Numerous reports exist in the literature where molecular orientation has been determined for surface-confined molecules; the techniques most frequently employed are linearly-polarized infrared (IR) absorbance spectroscopy,^{11,16–18,26–29} ultraviolet–visible (UV–vis) polarized absorbance spectroscopy (transmission,^{8,12,13,15,30–33}

or attenuated total reflection (ATR)),^{34–39} or polarized fluorescence spectroscopy.^{40–43} To fully describe the molecular orientation, a particular orientation of the transition dipoles with respect to the molecular structure is generally assumed and measurements of optical anisotropy are then used to determine an order parameter. For **Pc 1**, as well as for most metalated Pcs and porphyrins, introduction of the central metal gives the molecule D_{4h} symmetry, with two equivalent orthogonal electronic transition dipoles (μ_1 and μ_2) in the plane of the molecule (Figure 1a).^{30,31,44–47} Such molecular symmetry dictates a circular symmetry for optical absorption within the molecular plane. In most cases, this symmetry is considered to be maintained upon Pc aggregation or crystallization; however, it has been demonstrated for a number of Pcs that the electronic transition dipoles may be perturbed and that D_{4h} symmetry can be broken.^{46–48} For these cases, aggregation generally results in nonequivalent intensities and frequencies for μ_1 and μ_2 with predicted differences in electronic absorption wavelength as large as 15 nm. These transition dipoles generally remain within the molecular plane in such assemblies, yet may become offset from their original orientation within the molecular plane.⁴⁹

For most orientation studies, the treatment of optical anisotropy has been simplified by assuming a uniaxial molecular distribution, where two of the three experimental axes are effectively equivalent (e.g., the molecules are isotropically distributed about the substrate normal axis). Furthermore, most of these studies examined molecules with linearly-polarized electronic transition dipoles,^{27–29,34,35,43} where the theoretical treatment is simplified to an even greater extent. For example, Debe characterized uniaxial surfactant molecules with linearly-polarized vibrational transition dipoles on an aluminum surface using reflection–absorption infrared spectroscopy (RAIRS).²⁹ Cropek and Bohn determined the molecular

(27) Allara, D. L.; Nuzzo, R. G. *Langmuir* **1985**, *1*, 52.

(28) Parikh, A. N.; Allara, D. L. *J. Chem. Phys.* **1992**, *96*, 927.

(29) Debe, M. K. *Appl. Surf. Sci.* **1982**, *14*, 1.

(30) Frackowiak, D.; Ion, R.-M.; Waszkowiak, A. *J. Phys. Chem. B* **2002**, *106*, 13154.

(31) Hofrichter, J.; Eaton, W. A. *Ann. Rev. Biophys. Bioeng.* **1976**, *5*, 511.

(32) Yoneyama, M.; Sugi, M.; Saito, M.; Ikegami, K.; Kuroda, S.; Iizima, S. *Jpn. J. Appl. Phys., Part 1* **1986**, *25*, 961.

(33) Yan, W.; Zhou, Y.; Wang, X.; Chen, W.; Xi, S. *J. Chem. Soc., Chem. Commun.* **1992**, 873.

(34) Cropek, D. M.; Bohn, P. W. *J. Phys. Chem.* **1990**, *94*, 6452.

(35) Edmiston, P. L.; Lee, J. E.; Wood, L. L.; Saavedra, S. S. *J. Phys. Chem.* **1996**, *100*, 775.

(36) Doherty, W. J., III; Donley, C. L.; Armstrong, N. R.; Saavedra, S. S. *Appl. Spectrosc.* **2002**, *56*, 920.

(37) Edmiston, P. L.; Lee, J. E.; Cheng, S.-S.; Saavedra, S. S. *J. Am. Chem. Soc.* **1997**, *119*, 560.

(38) Lee, J. E.; Saavedra, S. S. In *Proteins at Interfaces II: Fundamentals and Applications*; Horbett, T. A., Brash, J. L., Eds; American Chemical Society: Washington, DC, 1995; p 269.

(39) Lee, J. E.; Saavedra, S. S. *Langmuir* **1996**, *12*, 4025.

(40) Bos, M. A.; Kleijn, J. M. *Biophys. J.* **1995**, *68*, 2566.

(41) Bos, M. A.; Kleijn, J. M. *Biophys. J.* **1995**, *68*, 2573.

(42) Fraaije, J. G. E. M.; Kleijn, J. M.; Van der Graaf, M.; Dijt, J. C. *Biophys. J.* **1990**, *57*, 965.

(43) Thompson, N. L.; McConnell, H. M.; Burghardt, T. P. *Biophys. J.* **1984**, *46*, 739.

(44) Gouterman, M. Part A. Physical Chemistry. In *The Porphyrins*; Dolphin, D., Ed.; Academic Press: New York, 1978; Vol. III, p 1.

(45) Stillman, M. J.; Nyokong, T. Absorption and Magnetic Circular Dichroism Spectral Properties of Phthalocyanines. In *Phthalocyanines: Properties and Applications*; Lever, A. B. P., Ed.; VCH: New York, 1989; Vol. 1, p 133.

(46) Mizuguchi, J. *J. Phys. Chem. A* **2001**, *105*, 1121.

(47) Lever, A. B. P. *Advances in Inorganic Chemistry and Radiochemistry*; Emelús, H. J., Sharpe, A. G., Eds.; Academic Press: New York, 1965; Vol. 7, p 27.

(48) Endo, A.; Matsumoto, S.; Mizuguchi, J. *J. Phys. Chem. A* **1999**, *103*, 8193.

(25) Drager, A. S.; O'Brien, D. F. *J. Org. Chem.* **2000**, *65*, 2257.

(26) Sauer, T.; Arndt, T.; Batchelder, D. N.; Kalachev, A. A.; Wegner, G. *Thin Solid Films* **1990**, *187*, 357.

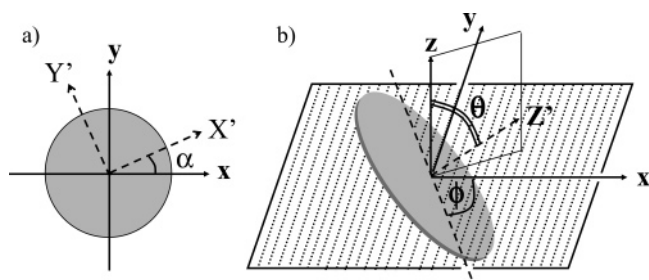


Figure 2. Coordinate system and schematic for describing angular orientation in discotic molecules: (a) α represents a rotation in the molecular plane of the electronic transition dipoles (along X' and Y' axes), away from the x axis of the lab coordinate system, (b) θ is a polar angle representing a tilt of the molecular dipole plane away from the x - y (substrate) plane (or a tilt angle between the molecular plane normal (Z' axis) and the substrate normal (z axis)), and ϕ is an azimuthal angle representing a rotation of the molecular plane about the z axis, away from the x axis.

orientation of uniaxial monolayers of monophenyl dimethylsilanes, using ATR UV-vis spectroscopy, with electronic transition dipoles treated as linearly polarized.³⁴ Allara and co-workers used a transfer-matrix formalism to determine orientations of uniaxial, linearly-polarized n -alkanoic acids and thiols on metal surfaces by comparing theoretical and experimental RAIRS spectra.^{27,28} The assumption of a uniaxial sample cannot be applied, however, to many types of molecular assemblies such as compressed LB films of liquid crystals, where molecules are not expected to be isotropically oriented about the normal of the sample plane and must be treated with a biaxial symmetry.

Linearly-polarized spectroscopic techniques have also been used to study discotic molecules.^{11-13,16-18,30-32,34-38} To define the orientation of a discotic molecule in space, three Euler angles are necessary. For the sake of a consistent discussion with previous studies, we adopt the coordinate system used by Bos and Kleijn⁴⁰⁻⁴² depicted in Figure 2, where α is a rotation angle along the normal of the molecular plane, θ is a tilt angle of the molecular plane away from the x - y (substrate) plane, and ϕ is an azimuthal rotation angle about the z axis. We assume that a D_{4h} in-plane symmetry results in a circular dipole in the molecular plane (circular absorber).^{11-13,15,30-32,36,39,42} Of the reports that have treated discotic molecules, many have also made the assumption of an isotropic distribution of orientations about ϕ , which again reduces the problem to a description of a uniaxial film and greatly simplifies the experimental and theoretical approaches for finding θ .^{30,31,36-42} This assumption is reasonable for many systems where molecules are surface confined with no director for order about ϕ , e.g. porphyrin-containing proteins (cytochrome *c*) adsorbed to various substrates.^{37,38,40-42} For more-dense or compressed films of discotic materials, including highly symmetric liquid crystalline materials, however, order often exists about the angle ϕ .^{8,15-25}

When investigators have been unable to make the assumption of an isotropic distribution of the angle ϕ , almost every literature report of molecular orientation in discotic assemblies, including some of our own previous studies, has relied on assuming a fixed value for ϕ or θ in order to simplify the determination of the other angle.^{11,12,15-18,26} Wegner and co-workers,²⁶ examined thin films composed of silicon phthalocyanine disks that were cofacially polymerized through $-O-Si-O-$ bonds, forcing them to be completely upright ($\theta = 90^\circ$). Polarized transmission IR measurements provided a simple approach for determining ϕ of those thin-film arrays of

parallel rodlike polymers. Earlier reports from this group using linearly-polarized IR spectroscopy of films of **Pc 1** assumed either $\phi = 90^\circ$ (leading to a θ value of ca. 55°) or $\theta = 90^\circ$ (leading to $\phi = 63^\circ$).^{16,17} Such a priori assumptions of orientation in nonpolymerized discotic mesophases are questionable, and it is desirable to use an approach which requires no assumed values for either ϕ or θ . Manno et al.¹³ did measure θ and ϕ for LB films of other CuPc derivatives based on work by Yoneyama et al.,³² using polarized transmission UV-vis spectroscopy measurements, at varying incident angles with respect to the substrate plane. They report values of $62 \pm 5^\circ$ and $64 \pm 5^\circ$ for θ and ϕ , respectively, for an 80-bilayer film of Cu(II)-tetrakis(3,3-dimethylbutoxycarbonyl)phthalocyanine. However, their analysis does not account for differences in reflectance when an optical beam impinges the sample surface at an oblique angle of incidence with different polarizations, and the reported results are not conclusive.

We recently developed a simple and sensitive broadband ATR spectroscopic platform for characterization of ultrathin films of molecular assemblies.³⁶ As shown below, we transfer single bilayer films of **Pc 1** to this platform with the axis of the rodlike Pc aggregate either parallel to, or perpendicular to, the optical axis of the experiment and obtain full visible-wavelength spectra at both TE and TM polarizations. These experiments provide for a fuller description of the optical anisotropy in these films than has been possible previously and has led us to develop a new methodology that allows for the determination of anisotropy in both angles, ϕ and θ , without any a priori assumptions.

The characterization method we present here, although focused on **Pc 1**, is intended to be useable for the characterization of molecular anisotropy in any discotic liquid-crystalline material. From the ATR measurements of single-bilayer films of these materials, the ensemble average of the transition dipole components are determined for each principal axis of the molecular film. Next, those results are treated with a circular absorber model for describing the adsorbed molecules in an effort to recover order parameters of molecular orientation. We observe, however, that a truly circular model is unable to fully explain the experimental results, indicating that the transition dipoles are perturbed upon aggregation. Then, the utility of this approach to elucidate information about film structure, without applying a specific molecular model, is further demonstrated by either (a) changing the phenyl- versus methyl-termination ratio of silane surface modifiers on the substrate or (b) annealing the Pc film, immersing it in water, and then annealing again. The results of these studies complement recent X-ray reflectometry¹⁹ and RAIRS and transmission FT-IR studies,^{17,18} from which we conclude nearly the same microstructure for these Pc films as those shown here.

Theory

The laboratory Cartesian coordinate system and the notations used here are shown in Figure 3. The molecular film lies in the x - y plane, the ATR probe beam propagates in the x - z plane, and the Pc-aggregate rod axis is presumed to lie either along the x or y axis, depending upon film orientation during transfer. ATR spectroscopies have been well described by Harrick.⁵¹ The absorbance,

(49) Kobayashi, N.; Fukuda, T.; Ueno, K.; Ogino, H. *J. Am. Chem. Soc.* **2001**, *123*, 10740.

(50) Donley, C. Ph.D. Dissertation, University of Arizona, **2003**.

(51) Harrick, N. J. *Internal Reflection Spectroscopy*; Interscience Publishers: New York, 1967.

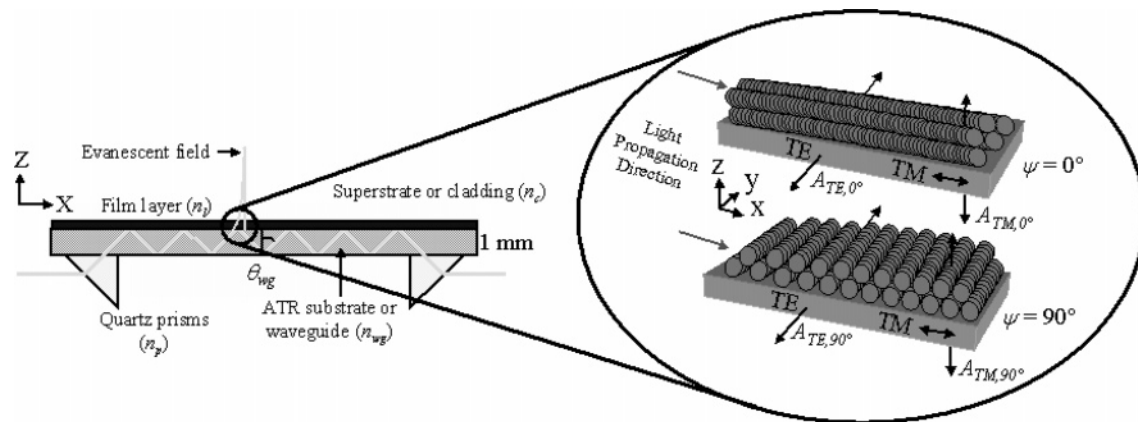


Figure 3. ATR measurement design. The laboratory coordinate system is defined such that the probe beam propagates in the $x-z$ plane. The recovery of molecular anisotropy is made possible by studying the sample at two orientations with respect to the probe beam at two different electric field polarizations. In TE polarization, the field is polarized in the y direction, and in TM polarization, the electric field has x and z components. The two sample orientations were selected such that the angles (ψ) between the molecular column direction and the x axis are 0° and 90° , respectively.

A , can be related to the molecular electronic transition dipole, $\vec{\mu}$, and the electric field, \vec{E} , by⁵²

$$A \propto \langle (\vec{\mu} \cdot \vec{E})^2 \rangle \quad (1)$$

where the brackets represent the ensemble average over the individual molecular dipole orientations. Later, the proportionality sign above is replaced by an equal sign, as the calculations to follow will involve only the ratio of absorbance values and any constant multiplying factor would be canceled out.

To determine the ensemble average of the squared dipole projections along the lab coordinate system, $\langle \mu_x^2 \rangle$, $\langle \mu_y^2 \rangle$, and $\langle \mu_z^2 \rangle$ (which, due to sample symmetry and alignment are the principal axes of the second-rank absorption dipole tensor),⁵³ we acquire absorbance measurements in TE and TM polarizations at two different sample orientations (Figure 3). We define ψ as the angle between the molecular column direction (which is collinear with the LB trough barriers and the presumed axis of the rodlike aggregates) and the x axis. In the initial sample orientation, the aggregate column axis is aligned along the x axis ($\psi = 0^\circ$); for the second sample, orientation the column axis is aligned along the y axis ($\psi = 90^\circ$). These measurements can be achieved at two distinct column orientations for materials which are coherent, mechanically durable, and provide for thin-film deposition in a way which preserves this orientation and coherence.^{5-8,17-21}

Expressions are written for the TE absorbance (A_{TE}) for the $\psi = 0^\circ$ sample orientation

$$A_{TE,0^\circ} \equiv \langle \mu_y^2 \rangle E_y^2 \quad (2)$$

and the $\psi = 90^\circ$ sample orientation

$$A_{TE,90^\circ} \equiv \langle \mu_x^2 \rangle E_y^2 \quad (3)$$

where E_y is the magnitude of the electric field along the y axis. By defining a ratio for the TE absorbance between the two sample orientations (r_{TE}), taking the ratio of

eq 2 to eq 3, an expression is obtained which is independent of E_y :

$$r_{TE} \equiv \frac{A_{TE,0^\circ}}{A_{TE,90^\circ}} = \frac{\langle \mu_y^2 \rangle}{\langle \mu_x^2 \rangle} \quad (4)$$

Expressions can also be given for the TM absorbance for the $\psi = 0^\circ$ sample orientation

$$A_{TM,0^\circ} \equiv \langle \mu_x^2 \rangle E_x^2 + \langle \mu_z^2 \rangle E_z^2 \quad (5)$$

and the $\psi = 90^\circ$ sample orientation

$$A_{TM,90^\circ} \equiv \langle \mu_y^2 \rangle E_x^2 + \langle \mu_z^2 \rangle E_z^2 \quad (6)$$

Equations 5 and 6 cannot be directly divided to remove the electric field intensities (E_x and E_z), as was the case for the TE measurements. However, in ATR experiments, E_x^2 and E_z^2 can be related to each other by the square of the magnetic field intensity (H_0^2) through the following relationships:⁵⁴

$$E_x^2 = \frac{(N_{TM}^2 - n_c^2)H_0^2}{(\epsilon_c c)^2} \quad (7)$$

$$E_z^2 = \left(\frac{n_c}{n_l}\right)^4 \frac{N_{TM}^2 H_0^2}{(\epsilon_c c)^2} \quad (8)$$

where n_c is the refractive index of the superstrate, n_l is the refractive index of the organic film, ϵ_c is the dielectric constant of the superstrate, c is the speed of light in a vacuum, and N_{TM} is the effective index of the waveguide, which is given by

$$N_{TM} = n_{wg} \sin \theta_{wg} \quad (9)$$

where n_{wg} is the refractive index of the ATR substrate waveguide (1.51 for glass) and θ_{wg} is the propagation angle of the probe beam in the substrate with respect to the substrate normal. Substituting eqs 7 and 8 into eqs 5 and 6 and then taking the ratio of these resultant expressions, we arrive at an expression that is independent of E_x and

(52) Hopf, F. A.; Stegeman, G. I. *Applied classical electrodynamics*; Wiley: New York, 1985; Vol. 1, p 29.

(53) Michl, J.; Thulstrup, E. W. *Spectroscopy with polarized light: solute alignment by photoselection, in liquid crystals, polymers, and membranes*; VCH: Deerfield Beach, FL, 1986.

(54) Kogelnik, H. Theory of Optical Waveguides. In *Guided-wave optoelectronics*, 2nd ed.; Alfness, R. C., Ed.; Springer-Verlag: New York, 1990; p 23.

E_z (and also of H_0) for the TM absorbance ratio for the two sample orientations (r_{TM}):

$$r_{\text{TM}} \equiv \frac{A_{\text{TM},0^\circ}}{A_{\text{TM},90^\circ}} = \frac{\langle \mu_x^2 \rangle (N_{\text{TM}}^2 - n_c^2) + \langle \mu_z^2 \rangle \left(\frac{n_c}{n_l}\right)^4 (N_{\text{TM}}^2)}{\langle \mu_y^2 \rangle (N_{\text{TM}}^2 - n_c^2) + \langle \mu_z^2 \rangle \left(\frac{n_c}{n_l}\right)^4 (N_{\text{TM}}^2)} \quad (10)$$

The sum of the average transition dipole components are related to the total dipole strength μ by

$$\langle \mu_x^2 \rangle + \langle \mu_y^2 \rangle + \langle \mu_z^2 \rangle = \mu^2 \quad (11)$$

Analytical solutions for $\langle \mu_x^2 \rangle / \mu^2$, $\langle \mu_y^2 \rangle / \mu^2$, and $\langle \mu_z^2 \rangle / \mu^2$, containing only the experimentally measured or known quantities (r_{TE} , r_{TM} , N_{TM} , n_c , and n_l), are obtained by combining eqs 4, 10, and 11:

$$\frac{\langle \mu_x^2 \rangle}{\mu^2} = \left[\left(\frac{n_c}{n_l}\right)^4 N_{\text{TM}}^2 (1 - r_{\text{TM}}) \right] / \left[\left(\frac{n_c}{n_l}\right)^4 N_{\text{TM}}^2 (1 + r_{\text{TE}} - r_{\text{TM}} - r_{\text{TE}} r_{\text{TM}}) + (n_c^2 - N_{\text{TM}}^2) (-1 + r_{\text{TE}} r_{\text{TM}}) \right] \quad (12)$$

$$\frac{\langle \mu_y^2 \rangle}{\mu^2} = \left[\left(\frac{n_c}{n_l}\right)^4 N_{\text{TM}}^2 (1 - r_{\text{TM}}) r_{\text{TE}} \right] / \left[\left(\frac{n_c}{n_l}\right)^4 N_{\text{TM}}^2 (1 + r_{\text{TE}} - r_{\text{TM}} - r_{\text{TE}} r_{\text{TM}}) + (n_c^2 - N_{\text{TM}}^2) (-1 + r_{\text{TE}} r_{\text{TM}}) \right] \quad (13)$$

$$\frac{\langle \mu_z^2 \rangle}{\mu^2} = [(n_c^2 - N_{\text{TM}}^2) (-1 + r_{\text{TE}} r_{\text{TM}})] / \left[\left(\frac{n_c}{n_l}\right)^4 N_{\text{TM}}^2 (1 + r_{\text{TE}} - r_{\text{TM}} - r_{\text{TE}} r_{\text{TM}}) + (n_c^2 - N_{\text{TM}}^2) (-1 + r_{\text{TE}} r_{\text{TM}}) \right] \quad (14)$$

By assuming a model relating the electronic transition dipoles to the molecular structure, one can then determine molecular orientation parameters using the results of eqs 12–14. Focusing on the optical absorption in the visible spectral region (ca. 625 nm), **Pc 1** can be modeled as a circular absorber with two equal and orthogonal transition dipoles and D_{4h} symmetry (Figure 1a) if we neglect any intermolecular interaction or any molecular deformation that could occur upon molecular aggregation. The Cartesian components of the electronic transition dipole vector in the molecular frame are translated into the lab coordinate system by an Euler rotation matrix transformation:

$$\begin{pmatrix} \mu_x \\ \mu_y \\ \mu_z \end{pmatrix} = \begin{pmatrix} \cos \phi & -\sin \phi & 0 \\ \sin \phi & \cos \phi & 0 \\ 0 & 0 & 1 \end{pmatrix} \begin{pmatrix} 1 & 0 & 0 \\ 0 & \cos \theta & -\sin \theta \\ 0 & \sin \theta & \cos \theta \end{pmatrix} \begin{pmatrix} \mu/\sqrt{2} \\ \mu/\sqrt{2} \\ 0 \end{pmatrix} \quad (15)$$

where μ is the magnitude of a transition dipole with equal components along the x and y axes of the molecular coordinate system. The rotation matrix in α provides a circular absorber if all α angles have the same probability. The rotation matrixes for θ and ϕ orient the molecular disk in space: θ is the angle between the molecular plane normal (Z' axis) and the sample surface normal (z axis)

and ϕ is the azimuthal rotation of the circular absorber about the z axis (Figure 2). The average values of the second-order components of the transition dipole, which are involved in the absorbance calculations, are determined by:⁵⁵

$$\langle \mu_i^2 \rangle = \frac{\int_0^{2\pi} d\alpha \int_0^{2\pi} d\phi \int_0^\pi \sin \theta d\theta \int_0^{2\pi} d\alpha N(\theta, \phi) \mu_i^2}{\int_0^{2\pi} d\alpha \int_0^{2\pi} d\phi \int_0^\pi \sin \theta d\theta \int_0^{2\pi} d\alpha N(\theta, \phi)} \quad (16)$$

with $i = x, y$, or z . Squaring the terms in eq 15 and integrating α over 0 to 2π , the following expressions relating the orientation parameters of a circular absorber and the experimentally determined transition dipole components are obtained:

$$\frac{\langle \mu_x^2 \rangle}{\mu^2} = \frac{1}{2} \{ \langle \cos^2 \phi \rangle + \langle \sin^2 \phi \cos^2 \theta \rangle \} \quad (17)$$

$$\frac{\langle \mu_y^2 \rangle}{\mu^2} = \frac{1}{2} \{ \langle \sin^2 \phi \rangle + \langle \cos^2 \phi \cos^2 \theta \rangle \} \quad (18)$$

$$\frac{\langle \mu_z^2 \rangle}{\mu^2} = \frac{1}{2} \langle \sin^2 \theta \rangle \quad (19)$$

These equations can then be solved to provide a solution for each order parameter. As is observed upon inspection of eqs 17–19, for a circular absorber, the maximum average value for each Cartesian component of the squared transition dipole normalized by the total dipole strength, $\langle \mu_i^2 \rangle / \mu^2$, is 1/2.

By analogous theoretical development, the molecular orientation parameters for the case of a molecule with a single, linear transition dipole are given by:⁵⁵

$$\frac{\langle \mu_x^2 \rangle}{\mu^2} = \langle \sin^2 \phi \sin^2 \theta \rangle \quad (20)$$

$$\frac{\langle \mu_y^2 \rangle}{\mu^2} = \langle \cos^2 \phi \sin^2 \theta \rangle \quad (21)$$

$$\frac{\langle \mu_z^2 \rangle}{\mu^2} = \langle \cos^2 \theta \rangle \quad (22)$$

where θ is the polar angle and ϕ is the azimuthal angle of the transition dipole vector. For this case, each Cartesian component, $\langle \mu_i^2 \rangle / \mu^2$, can span a wider range (0–1), while the condition is still satisfied that the sum over all components is equal to 1, per eq 11.

Experimental Section

ATR Substrate Preparation. ATR substrates were prepared by cleaning glass microscope slides (1 mm thickness) in Klean AR (Mallinckrodt) for 5 min. Substrates were rinsed with deionized water (18 M Ω) and dried in a stream of nitrogen. Unless otherwise indicated, the substrates were rendered hydrophobic by exposure to a 5.4% (v/v) solution of a disilazane mixture (50:50 (v/v) of 1,1,1,3,3,3-hexamethyldisilazane (HMDS) and 1,3-diphenyl-1,1,3,3-tetramethyldisilazane (DPTMDS) (Aldrich)) in CHCl_3 at $40 \pm 5^\circ \text{C}$ for 30 min, with stirring.^{17–19} Following

(55) Zanoni, C. Order Parameters and Orientational Distributions in Liquid Crystals. In *Polarized Spectroscopy of Ordered Systems*; Kluwer Academic Publishers: Norwell, MA, 1988, pp 57–83.

disilazane exposure, substrates were rinsed with CHCl_3 and dried in a stream of nitrogen.

Film Deposition and Annealing. Bilayer films of **Pc 1**,^{15–20} were prepared on a Langmuir–Blodgett (LB) trough (Riegler and Kerstein RK3).^{15–20} Following compression to a stable bilayer, the water subphase was evacuated until the Pc film was lowered onto an aluminum baffle, cutting it into discrete rectangular sections of coherent, single bilayers (ca. 5.6–6.0 nm thickness) of the material.²² Prior to film deposition on ATR substrates, half of the substrate was masked (along the optical axis) by clamping an unmodified glass slide over half of the substrate. This prevented film deposition on the masked portion, allowing its use as a spectroscopic blank.^{22,34–36} Single bilayer films of **Pc 1** were then horizontally transferred to the unmasked portion of the ATR substrate. Alignment of the molecular columns with respect to the substrate long axis (Figure 3) was controlled through the alignment of the substrate with respect to the trough barriers during deposition. This was facilitated by the baffle, which was machined to give rectangular deposition zones, rotated 0° and 90° with respect to the trough barriers.²² Following film deposition, coated substrates were dried in a stream of nitrogen and stored in a desiccator or immediately annealed in a vacuum oven at 10^{-6} Torr and 120°C for 3 h in order to remove any residual water and move the sample up through its liquid-crystal transition temperature (ca. 68°C) and back, which improves ordering.^{17–22} Films were then stored in a desiccator until further analysis.

Spectroscopic Analysis of Films by UV–Vis ATR. The recently described broadband UV–visible attenuated total internal reflectance (ATR) instrument was used here with only minor modifications.³⁶ The broadband coupling capability, and the CCD detection make it possible to acquire thin-film spectra across the full visible region with acquisition times under 3 s per spectrum. The probe beam was coupled in and out of the ATR cell with two 45° – 90° fused silica prisms ($n_p = 1.46$), spaced 39.7 mm apart on the backside of the glass substrate ($n_{wg} = 1.51$), using index matching fluid ($n = 1.48$). Analysis was carried out at a coupling angle of 33.92° between the prism surface normal and the impinging light beam, producing a substrate propagation angle (θ_{wg}) of 63.27° , which is significantly higher than the critical angle (41.5°), resulting in 10 reflections of the probe beam in the ATR platform. N_{TM} values were calculated according to eq 9 using the n_{wg} and θ_{wg} values listed above.

Measurement of Film Refractive Index. Refractive index (n_i) measurements were made on nine-bilayer films of **Pc 1** deposited on a chemically modified gold surface using a Sentech 400 discrete wavelength (He–Ne, 633 nm), multiple-angle ellipsometer. Nine-bilayer films were chosen to give target thicknesses of approximately 50 nm, which is sufficient to give unambiguous instrumental response. Cleaned Au substrates were chosen to give high contrast between the refractive index of the substrate and the film⁵¹ and were modified through exposure to a 1 mM solution of benzyloxyethanethiol in ethanol for 24 h to provide for coherent Pc films.^{16–20} Real (n) and imaginary (k) substrate optical constants were measured for unmodified Au at an incident angle of 70° with respect to the substrate normal. The film refractive index, n_i , was measured (treating the thiol and Pc film as a single layer) by collecting Ψ and Δ values at 70° , 65° , and 60° with the Pc columns aligned in the plane of incidence. Using the measured substrate optical constants, k_i was calculated iteratively until the root-mean-square of n_i for the three angles was minimized.

Treatment of Raw ATR Data. Each set of three ATR spectra was averaged to give one representative raw spectrum in TE and TM modes for the blank and the **Pc 1**-coated regions of the substrate. Absorbance spectra were calculated from the dark-subtracted blank and film transmission spectra. Values for $\langle\mu_i^2\rangle/\mu^2$ were then calculated using eqs 12–14 at the peak absorbance (~ 625 nm) with the measured values of r_{TE} , r_{TM} , N_{TM} , and n_i described above and the refractive index of air ($n_c = 1.00$).

Transmission UV–Vis Measurements. Transmission UV–vis absorbance spectra were collected using a customized sampling bench attachment for an SI 400 fiber-optic spectrophotometer (Spectral Instruments, attachment provided by manufacturer), which accommodates a polarizer and a thin-film holder in the optical axis.²² **Pc 1** films (1 and 4 bilayer) on 50:50

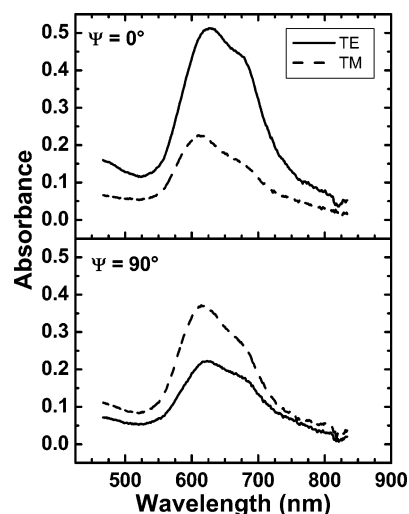


Figure 4. ATR spectra for a single annealed bilayer of **Pc 1** on modified (50:50 DPTMDS/HMDS) glass for two sample orientations.

DPTMDS:HMDS modified glass were analyzed, with the sample plane perpendicular to the incident beam. Incident radiation was linearly polarized at various angles (γ) within the sample plane, with respect to the molecular column direction. Blank spectra were acquired for a clean glass substrate at each polarization and subtracted from film spectra.

Results and Discussion

ATR Absorbance Spectra. ATR absorbance spectra for a single annealed bilayer of **Pc 1** on modified (50:50 DPTMDS:HMDS) glass in air are presented in Figure 4 for two sample orientations. Qualitative information about the molecular orientation in this sample is inferred by relating these TE and TM absorbance spectra to the measurement geometries defined in the Theory section and in Figure 3 above. For the TE spectra (electric field along the y axis), the absorbance is much higher for the $\psi = 0^\circ$ sample orientation than for the $\psi = 90^\circ$ sample orientation, suggesting that a higher population of transition dipoles within the molecular plane are oriented perpendicular to, rather than parallel to, the Pc aggregate column axis. For the TM spectra (electric field along the x and z axes), a slightly larger absorbance is observed for the $\psi = 90^\circ$ sample orientation. The anisotropy in TM absorbance is solely due to the dipole components in the sample plane, since the z component does not change with sample rotation about the z axis. Therefore, a TM absorbance that is higher at $\psi = 90^\circ$ than at $\psi = 0^\circ$, but with a smaller anisotropy compared to the TE ($\psi = 0^\circ$ versus $\psi = 90^\circ$) spectra, is consistent with the previous conclusion for measurements made with TE polarization.

Average absorbance ratios, $r_{\text{TE}} = 2.5 \pm 0.2$ and $r_{\text{TM}} = 0.63 \pm 0.05$, were computed from characterization of at least three separate bilayer films. Absorbance ratios and transition dipole components for all samples studied are presented in Table 1. Table 1 also includes the expected values for an entirely random sample (in a perfectly random sample, r_{TE} and r_{TM} are unity).

Anisotropy Parameters. Transition dipole components, $\langle\mu_i^2\rangle/\mu^2$, were calculated using eqs 12–14 as described in the Theory section, utilizing a measured value $n_i = 1.66$ for these **Pc 1** bilayers, which is comparable to $n_i = 1.70$ reported for LB films of a similarly substituted CuPc.¹³ When each sample set is treated independently, average values are obtained for $\langle\mu_x^2\rangle/\mu^2$, $\langle\mu_y^2\rangle/\mu^2$, and $\langle\mu_z^2\rangle/\mu^2$ of 0.12 ± 0.04 , 0.30 ± 0.08 , and 0.6 ± 0.1 , respectively. For an entirely random sample, each of these parameters

Table 1. Absorbance Ratios and Dipole Components

sample set ^a	r_{TE}	r_{TM}	$\langle\mu_x^2\rangle/\mu^2$	$\langle\mu_y^2\rangle/\mu^2$	$\langle\mu_z^2\rangle/\mu^2$
standard - 1	2.63	0.69	0.08	0.21	0.71
standard - 2	2.56	0.59	0.13	0.33	0.54
standard - 3	2.24	0.61	0.16	0.35	0.49
average \pm standard deviation	2.5 ± 0.2	0.63 ± 0.05	0.12 ± 0.04	0.30 ± 0.08	0.6 ± 0.1
random ^b	1	1	1/3	1/3	1/3
Environmental Exposure					
as deposited	2.26	0.49	0.25	0.56	0.19
annealed (same as "standard - 1")	2.63	0.69	0.08	0.21	0.71
after water exposure	2.38	0.66	0.11	0.27	0.62
reannealed	2.66	0.74	0.06	0.16	0.77
Surface Pretreatment (% Phenyl Silane Modifier)					
0	2.51	0.51	0.18	0.46	0.36
25	2.40	0.52	0.20	0.47	0.33
50 (same as average standard sample)	2.48	0.63	0.12	0.30	0.58
100	2.99	0.53	0.12	0.36	0.52

^a Sample is 1 bilayer **Pc 1** on 50:50 HMDS/DPTMDS modified glass, annealed, unless otherwise indicated. ^b Theoretical values for a sample where the ensemble orientation is totally randomized.

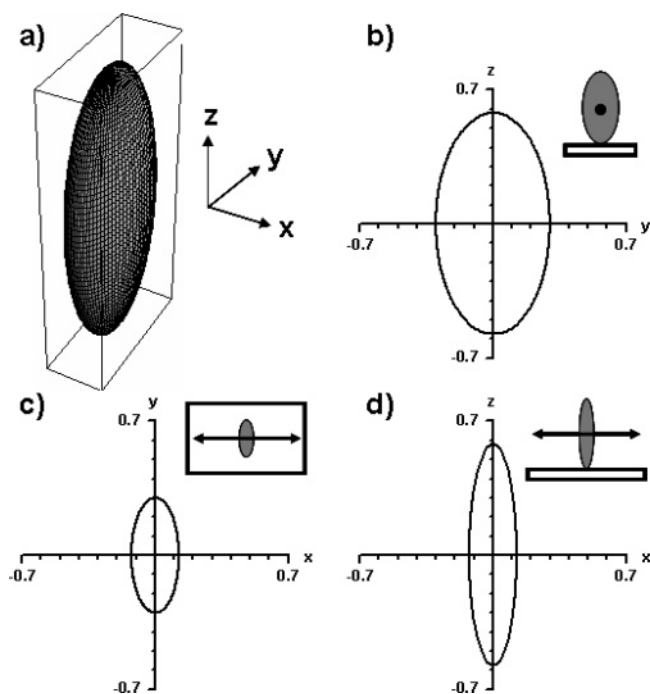


Figure 5. Schematic representation of dipole strength along each Cartesian component. An ellipsoid with each axis proportional to the transition dipole strength, $\langle\mu_i^2\rangle/\mu^2$, provides a visual representation (a) in a three-dimensional plot and (b–d) in two-dimensional cross-sections.

would be theoretically equal to 1/3. Thus, the experimental results confirm that the individual Pc dipoles are (a) highly oriented along the normal axis of the ATR substrate (z axis) and (b) for the in-plane (x – y) distribution, are more aligned along the y axis (perpendicular to the rodlike aggregate column direction; see Figure 3), based on a ratio of 2.5 ± 0.2 for $\langle\mu_y^2\rangle/\langle\mu_x^2\rangle$. These results are illustrated in Figure 5, where an ellipsoid with a semi-axis proportional to the Cartesian dipole components provides a visualization of its strength along each direction.

Next, we observe that the average value of the z component of the transition dipole, $\langle\mu_z^2\rangle/\mu^2$, is 0.6 ± 0.1 , with a single value as high as 0.71 determined for one of the three sample sets evaluated. These results are inconsistent with a circular absorber model (where the maximum theoretical value is 1/2 for any Cartesian component of the transition dipole) for **Pc 1**. In other words, the value of $\langle\mu_z^2\rangle/\mu^2$ shows a preferential alignment of the transition dipoles perpendicular to the sample plane

that is greater than what could be obtained by an ensemble of circular absorbers uniformly aligned upright on the sample surface. The wavelength positions of the absorbance peaks in the ATR spectra shown in Figure 4 provide additional insight. For the TE spectra, the peak wavelength at both sample orientations are similar; however, the peaks in the TM spectra are consistently blue-shifted with respect to the TE spectra by ca. 10 nm. This result suggests that a z component of the transition dipole is centered at a shorter wavelength compared to its x and y counterparts. Taken together, these observations suggest that compact aggregation of **Pc 1** in the LB bilayer film is accompanied by a slight geometrical perturbation of the macrocyclic core, leading to a perturbation of the μ_1 and/or μ_2 frequencies. Such splitting of the optical symmetry is also expected to create unequal μ_1 and μ_2 dipole strengths.^{44–46} Such perturbations are more typically seen for phthalocyanines which have been asymmetrically substituted, especially at nonperipheral positions.⁴⁹ Annealed thin film aggregates of the type emanating from our recent work, however, have not been extensively explored, and unless the kind of spectroscopic anisotropies shown here were specifically evaluated, it would not be apparent that such distortions of the macrocycle had occurred.

In-Plane Anisotropy by Polarized UV-Vis Transmission Spectroscopy. In-plane anisotropy was independently investigated by polarized transmission UV-visible absorbance experiments, which were carried out on one- and four-bilayer films. A schematic demonstrating how this measurement was made is presented in the inset of Figure 6. By measuring the absorbance with the electric field polarized at several directions in the x – y plane, a direct measurement of the transition dipoles projection can be obtained. Peak absorbances were measured as a function of polarization angle (in the sample plane, referenced to the molecular column direction) and are accordingly plotted in Figure 6. The largest absorbance measured was observed at a polarization angle of ca. 90° for both the one- and four-bilayer samples (perpendicular to the rodlike aggregate column axis), which confirms that the principal axes of the absorption tensor are along the axes of the Cartesian coordinate system depicted in Figure 3. The signal-to-noise ratio in the one-bilayer sample was poor, yet large enough to determine a polarization angle of maximum absorbance of $93 \pm 10^\circ$. The four-bilayer sample produced an equivalent result at a greater signal-to-noise ratio ($90 \pm 5^\circ$), which indicates that the in-plane orientation of bilayers 2–4 are not significantly different

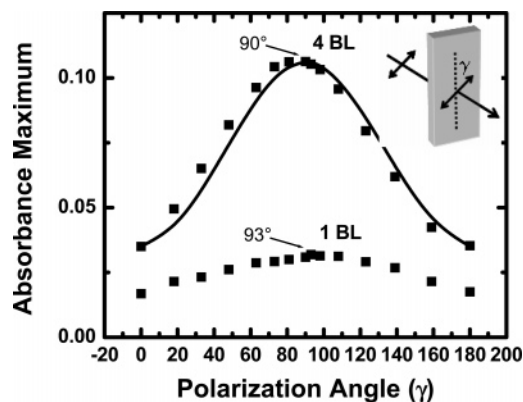


Figure 6. Polarized transmission UV-vis peak absorbances for one- and four-bilayer **Pc 1** films annealed on modified glass (50:50 DPTMDS/HMDS) as a function of γ , the in-plane polarization angle with respect to the column axis. The solid line is a theoretical fitting of absorbance versus polarization angle assuming dipole strength values along and perpendicular to the column direction.

from the first bilayer. The in-plane anisotropy, $\langle \mu_y^2 \rangle / \langle \mu_x^2 \rangle$, measured by the UV-vis transmission is ca. 3, which agrees reasonably with the ATR experimental result (2.5).

Further Applications: Effects of Environmental Conditions and Surface Modification on Molecular Anisotropy. The instrumentation and theory for measurement of molecular anisotropy described above were employed to monitor structural changes in **Pc 1** films. The results for the first study are listed in Table 1 and summarized in Figure 7a—anisotropy for a **Pc 1** bilayer on modified (50:50 DPTMDS:HMDS) glass was monitored in air for (a) the as-deposited film, (b) after annealing of this film above the $K \rightarrow LC$ mesophase transition temperature for this material and then re-cooling to R.T., (c) after immersing this film in water for ca. 30 min and drying in a desiccator, and finally (d) after repeating the above annealing cycle. The ratio of the in-plane dipole components shows relatively little variation (2.3–2.7) over steps (a–d). In contrast, upon annealing, the z component of the film changed significantly (from 0.18 to 0.71). Assuming μ_1 and μ_2 remain in the molecular plane upon aggregation of **Pc 1** in a LB film, the data show that prior to annealing the molecules are almost exclusively rotated perpendicular to the column direction and are substantially tilted over toward the substrate plane (small z component). Upon annealing, which is the case described in greater detail above, the molecules acquire a stronger z component absorbance and an almost exclusively upright orientation. During the annealing process, it is believed that the molecules have sufficient mobility to reorient into a more-stable, ordered configuration.^{18–20} Subsequent exposure of the sample to water does appear to cause some structural changes, which are likely due to incorporation of water into the ethylene oxide side chain regions; however, the subsequent annealing step returns the film to the microstructure seen after the first annealing step.

In a second study, we evaluated the orientation of a single annealed bilayer of **Pc 1** in air as a function of the composition of silane coating applied to the substrate prior to LB deposition. The percent methyl- versus phenyl-termination of silane-modified silica surfaces has been previously shown, using X-ray reflectometry, to alter the apparent tilt angle of the **Pc** disks and the side chains,¹⁹ and these modifications have also been shown to change the polarized IR absorbance anisotropy in two molecular directions (along versus perpendicular to column axis) for this material^{17,19,20} but have not been correlated to changes

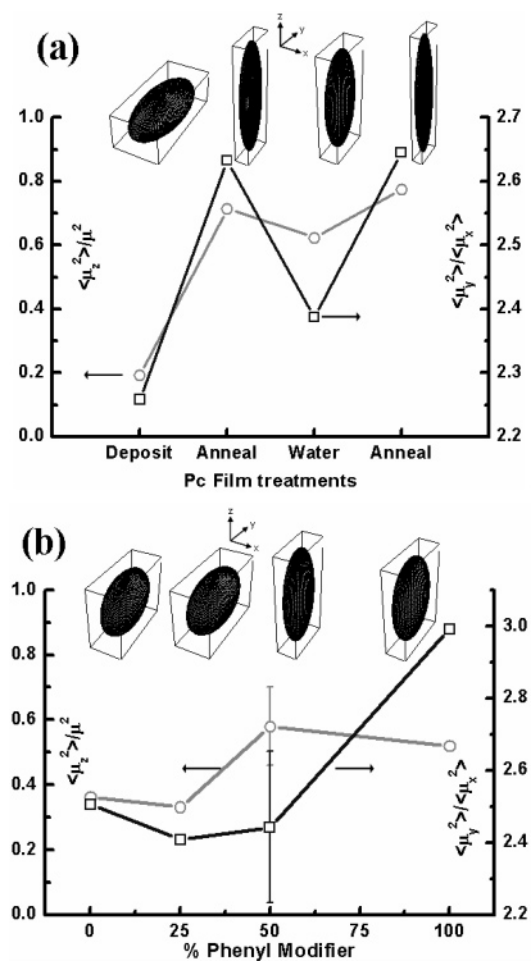


Figure 7. Molecular anisotropy as a function of (a) chronological environmental exposures applied to one sample and (b) fraction of phenyl groups used for the substrate surface modification prior to **Pc 1** film deposition.

in other anisotropic properties of the film. For the studies reported here, ATR substrates were modified with a mixture of varying volume fractions of diphenyltetramethylsilazane (DPTMDS) and hexamethyldisilazane (HMDS), producing substrates with varying relative surface phenyl concentrations. Resultant absorbance ratios and anisotropy parameters for these samples are listed in Table 1 and are also plotted in Figure 7b. The alignment along the z component shows a critical behavior for surface concentrations of phenyl groups produced using 25–50% of DPTMDS in the silane-modifier mixture. Below this concentration, a lower level of alignment along the z axis is observed, and above this concentration, a significantly greater alignment takes place. The in-plane ratio of the dipole components shows a smaller but noticeable (2.5–3.0) change between 50% and 100% of DPTMDS in silane-modifier mixture. These results are entirely consistent with both previous IR studies^{17,18} and the more-recent X-ray reflectometry studies.¹⁹

On the basis of these studies, it is hypothesized that the **Pc 1** molecules do not sit upright upon initial LB deposition. Once annealed, if the proper silane modification of the substrate has occurred (e.g., large concentrations of phenyl-terminated silanes), the molecules adopt a more-upright orientation. Stabilizing intermolecular interactions, such as π - π overlap between the phenyl groups at the **Pc** periphery and the surface phenyls, may facilitate this orientation change upon annealing, especially at high surface phenyl concentrations where the

additive effect of these interactions is presumably greater. Once annealed, this new molecular orientation is relatively stable with regard to the environmental exposures studied. In contrast, the in-plane anisotropy, with relatively smaller changes (2.5–3.0) in response to annealing and water exposure, seems to be predominantly established at the time of the film formation.

Conclusions

Most previous reports of techniques for measuring molecular tilt and azimuthal rotation in films of discotic mesophase materials have relied on making a priori assumptions as to the mean value (or isotropic nature) of one of these angles to determine the other. Here, we have presented an ATR method for fully describing molecular anisotropy (orientation) for these systems, where those assumptions are not needed. The approach was targeted at such materials as liquid crystals, where appreciable order is expected within rodlike columnar aggregates. Our results indicate that, although **Pc 1** molecules have D_{4h} symmetry, a circular dipole model is unable to explain the experimental data, suggesting that aggregation distorts the circular symmetry of the isolated molecule.

These studies also illustrate the use of polarized UV–vis ATR to investigate relative changes in the orientation of surface-confined discotic molecules. Although this study

focused on discotic liquid crystals, the technique is not limited to such systems and may be directly applied to a variety of films, including multiple layers and thick films. Although we studied a bilayer here because of the enhanced rigidity of this film, thinner and/or more weakly absorbing films may be investigated as well. We estimate the limit of detection to be 0.003 absorbance units,^{22,36} or 0.05 monolayers for molecules such as Pc's, with high molar absorptivities ($\epsilon > 10^5 \text{ M}^{-1} \text{ cm}^{-1}$), facilitating the unambiguous study of submonolayer films or interfacial layers, in addition to bulk analysis.

Acknowledgment. This work was supported in part by the National Science Foundation (N.R.A., Chemistry-0211900; S.S.S., Chemistry-0108805), the Office of Naval Research (N.R.A.), and the NSF Science and Technology Center-Materials and Devices for Information Technology DMR-0120967. We thank Rebecca Zangmeister for the acquisition of the AFM image presented in Figure 1. W.H.F. gratefully acknowledges the Pfizer Pharmaceuticals Graduate Research Fellowship in Analytical Chemistry for fellowship support. W.J.D. acknowledges fellowship support from the Proposition 301 Graduate Fellowship in Photonics.

LA0480078